Biotechnology Reports 33 (2022) e00697

Contents lists available at ScienceDirect

Biotechnology Reports

journal homepage: www.elsevier.com/locate/btre

Increased expression of the fluorescent reporter protein ymNeonGreen in *Saccharomyces cerevisiae* by reducing RNA secondary structure near the start codon.

Ronald E. Hector [a,*], Jeffrey A. Mertens [a], Nancy N. Nichols [a]

[a] *USDA, Agricultural Research Service, National Center for Agricultural Utilization Research, Bioenergy Research Unit, 1815 North University Street, Peoria, IL 61604, USA*

ARTICLE INFO

Keywords:
Saccharomyces
Green fluorescent protein
Ymneongreen
Secondary RNA structure
Translation
ymNeonGreen

ABSTRACT

Expression of a new fluorescent reporter protein called mNeonGreen, that is not based on the jellyfish green fluorescent protein (GFP) sequence, shows increased brightness and folding speed compared to enhanced GFP. However, *in vivo* brightness of mNeonGreen and its yeast-optimized variant ymNeonGreen in *S. cerevisiae* is lower than expected, limiting the use of this high quantum yield, fast-folding reporter in budding yeast. This study shows that secondary RNA structure near the start codon in the ymNeonGreen ORF inhibits expression in *S. cerevisiae*. Removing secondary structure, without altering the ymNeonGreen protein sequence, led to a 2 and 4-fold increase in fluorescence when expressed in *S. cerevisiae* and *E. coli*, respectively. In *S. cerevisiae*, increased fluorescence was seen with strong and weak promoters and led to higher transcript levels suggesting greater transcript stability and improved expression in the absence of stable secondary RNA structure near the start codon.

1. Introduction

Fluorescent reporter proteins such as the green fluorescent protein (GFP), originally identified from jellyfish, *Aequorea victoria*, have been improved upon over the last two decades making them very useful as markers for gene expression [1,2]. Among the properties improved are, generating a single emission wavelength, increased brightness, shifted emission wavelength, increased speed of folding, codon adaptation for improved expression, and monomerization (Table 1).

While GFP based on *A. victoria* has been vastly improved, relatively low overall brightness and slow maturation time still limit its usefulness as a reporter for low abundance proteins or fast-changing gene expression patterns. Additional fluorescent proteins (FPs) have been isolated and characterized in efforts to overcome these issues. One of these newer FPs, LanYFP, is a tetrameric yellow fluorescent protein from *Branchistoma lanceolatum* that is 4-fold brighter than enhanced GFP (EGFP). mNeonGreen, a monomerized GFP based on LanYFP, is 2.7-fold brighter than EGFP with an estimated maturation time of less than 10 min [7]. Consistent with this report, mNeonGreen protein maturation time measured in *Drosophila melanogaster* was about 7 min [10]. Faster folding of this fluorescent protein is expected to increase the temporal resolution of fast-changing gene expression systems. mNeonGreen has also been shown to express well in mammalian cells and localize correctly when expressed as C- or N-terminal fusions. Expression of mNeonGreen in *Caenorhabditis elegans* showed 3–5 fold more fluorescence than GFP optimized for expression in *C. elegans* [11] and a codon-optimized form of mNeonGreen based on human codon usage was 1.4 fold brighter in mammalian cells than the non-optimized mNeonGreen [12]. mNeonGreen expression was also characterized in budding yeast, *Saccharomyces cerevisiae,* against 26 other fluorescent proteins. Among GFPs, mNeonGreen was identified as the brightest when normalized to an equimolar control FP [8]. However, overall expression of mNeonGreen in *S. cerevisiae* was low, although the codon-optimized mNeonGreen ($ymNeonGreen_{WT}$) was able to increase fluorescence by ~25% [8]. Additional studies of the $ymNeonGreen_{WT}$ variant also showed *in vivo* brightness to be much lower than expected based on its *in vitro* properties [13] and *in vivo* fluorescence when expressed in additional cell lines and microorganisms. A possible

[§]Mention of trade names or commercial products in this publication is solely for the purpose of providing specific information and does not imply recommendation or endorsement by the U.S. Department of Agriculture. USDA is an equal opportunity provider and employer.

* Corresponding author.
E-mail address: Ronald.Hector@usda.gov (R.E. Hector).

https://doi.org/10.1016/j.btre.2021.e00697
Received 20 September 2021; Received in revised form 22 December 2021; Accepted 27 December 2021
Available online 31 December 2021

explanation for the poor fluorescence of mNeonGreen and ymNeonGreen$_{WT}$ in *S. cerevisiae* compared to other organisms is the presence of inhibitory RNA structure in the mRNA. Stable mRNA secondary structures are known to inhibit translation in both prokaryotes and eukaryotes [14–17]. In eukaryotes, there are differences in the magnitude of effect that mRNA hairpin structures exert on translation [18]. While translation in mammalian cells can proceed uninhibited through an RNA hairpin with $\Delta G = -30$ kcal/mol [16], translation in *S. cerevisiae* can be inhibited considerably by hairpin structures in the 5′ UTR with folding stabilities around −10 kcal/mol [18–21]. Analysis of the mRNA structure around the start codon of ymNeonGreen$_{WT}$ showed the presence of an RNA hairpin with a folding energy of −14.50 kcal/mol (see Materials and Methods). In this study, we reduced mRNA structure stability near the start codon while keeping the original protein sequence unaltered. The effect of mRNA structure on fluorescence of ymNeonGreen in *S. cerevisiae* and *Escherichia coli* is reported.

2. Materials and methods

2.1. Strains, media, statistics, and general methods

Media preparation, cell growth, transformation, and statistical analyses were performed as previously described [22]. All plasmids and microorganisms used in this study are listed in Tables 2 and 3, respectively.

2.2. Plasmid construction

Plasmids pRH908, pRH922, pRH927, pRH929, pRH930, pRH932, and pRH933 were constructed using pRH164 as the parent. Plasmid pRH164 was digested with *BssH*II and the NEBuilder HiFi DNA Assembly kit (NEB; Ipswich, MA, USA) was used to join DNA fragments to the parent vector. The DNA fragments used in this study were designed to include a promoter, fluorescent protein ORF, and transcription termination sequence, and are described in more detail in supplemental material. All DNA fragments were purchased from Integrated DNA Technologies (IDT; Coralville, IA, USA). The *lac* promoter was used for testing expression in *E. coli*. It is part of the pRS shuttle vector series for *S. cerevisiae* plasmids [26]. The pRS series of plasmids are based on pBluescript, which contains the *lac* promoter driving expression of the *LacZ* alpha fragment to be used for blue/white screening for the presence of DNA fragments inserted at the multi-cloning site. Construction of plasmids with the *lac* promoter was performed by co-transformation of yeast with the DNA fragment containing the *lac* promoter, ymNeonGreen variant ORF, and terminator (see supplemental material for additional sequence and details) and the *BssH*II digested and purified vector. Yeast recombinational repair was used to repair the digested plasmid using the co-transformed DNA fragment as a template. Two hundred nucleotides of homologous sequence on the ends of the DNA fragment were included to direct homologous recombination to the co-transformed digested plasmid. Plasmids with the *lac* promoter were rescued from yeast cells and transformed into *E. coli* for expression analysis. All plasmids were sequence-verified to confirm the inserted DNA fragments were correct prior to transformation into cells for fluorescence analysis.

Table 2
Plasmids used in this study.

Plasmid	Description	Source
pRS414	pBluescript II SK +, TRP1, CEN6, ARSH4	[23]
pRH164[a]	pRS414 + P_{HXT7} – MCS – T_{HXT7}	[24]
pRH908	pRS414 + P_{HXT7} – ymNeonGreen$_{WT}$ – T_{HXT7}	This work
pRH922	pRS414 + P_{HXT7} – yEGFP3 – T_{HXT7}	This work
pRH927	pRS414 + P_{HXT7} –ymNeonGreen$_{RM}$ – T_{HXT7}	This work
pRH929	pRS414 + P_{lac} – ymNeonGreen$_{WT}$ – T_{HXT7}	This work
pRH930	pRS414 + P_{lac} – ymNeonGreen$_{RM}$ – T_{HXT7}	This work
pRH932	pRS414 + P_{CYC1} – ymNeonGreen$_{WT}$ – T_{HXT7}	This work
pRH933	pRS414 + P_{CYC1} – ymNeonGreen$_{RM}$ – T_{HXT7}	This work

[a] The *HXT7* promoter (P_{HXT7}) used in this work refers to the truncated, constitutive promoter, containing 390 nucleotides upstream of the *HXT7* ORF [25]. RM designation refers to a ymNeonGreen variant with the same amino acid sequence as wild-type ymNeonGreen, but RNA modified (RM) to reduce mRNA structure from nucleotide 1 to 50 of the open reading frame.

Table 3
Microorganisms used in this study.

Strain	**Genotype (description)**	Source
NEB 5α	E. coli *fhuA2* D(*argF-lacZ) U169 phoA glnV44 f80D(lacZ)* M15 *gyrA96 recA1 relA1 endA1 thi-1 hsdR17*	NEB
CEN. PK2–1C	*S. cerevisiae MATa ura3–52 trp1–289 leu2–3,112 his3Δ1 MAL2–8^C SUC2*	Euroscarf
YRH1877	CEN.PK2–1C [pRH164 (empty vector control)]	This work
YRH1879	CEN.PK2–1C [pRH908 (pRS414 + P_{HXT7} –ymNeonGreen$_{WT}$ – T_{HXT7})]	This work
YRH1896	CEN.PK2–1C [pRH922 (pRS414 + P_{HXT7} – yEGFP3 – T_{HXT7})]	This work
YRH1897	CEN.PK2–1C [pRH929 (pRS414 + P_{lac} – ymNeonGreen$_{WT}$ – T_{HXT7})]	This work
YRH1898	CEN.PK2–1C [pRH930 (pRS414 + P_{lac} – ymNeonGreen$_{RM}$ – T_{HXT7})]	This work
YRH1900	CEN.PK2–1C [pRH927 (pRS414 + P_{HXT7} – ymNeonGreen$_{RM}$ – T_{HXT7})]	This work
YRH1902	CEN.PK2–1C [pRH932 (pRS414 + P_{CYC1} – ymNeonGreen$_{WT}$ – T_{HXT7})]	This work
YRH1903	CEN.PK2–1C [pRH933 (pRS414 + P_{CYC1} – ymNeonGreen$_{RM}$ – T_{HXT7})]	This work

Table 1
Properties of fluorescent reporter proteins.

Reporter	λ_{ex}	λ_{em}	ε ($mM^{-1}cm^{-1}$)	QY	Brightness	Association State	Maturation[a] (min)	Reference[b]
avGFP	395	509	25.0	0.79	19.75	Dimer	36	[3]
EGFP	488	507	55.9	0.60	33.6	Weak dimer	25	[4]
mEGFP[c]	488	507	55.9	0.60	33.6	monomer	25	[5]
GFPmut3	501	511	89.4	0.39	34.9	Weak dimer	25	[4]
yEGFP3[d]	501	511	89.4	0.39	34.9	Weak dimer	25	[6]
LanYFP	513	524	150	0.95	142.5	Tetramer	ND	[7]
mNeonGreen	506	517	116	0.80	92.8	Monomer	<10	[7]
ymNeonGreen[e]	506	517	116	0.80	92.8	Monomer	<10	[8]

Fluorescent reporter property definitions: Excitation peak (λ_{ex}), emission wavelength (λ_{em}), extinction coefficient (ε), quantum yield (QY). Brightness values represent the product of QY and ε.
[a]Time for fluorescence to reach its half-maximal value after exposure to oxygen at 37 °C.
[b]Table data supplemented from reference and data maintained in FPbase (https://www.fpbase.org/) [9].
[c]Properties from EGFP.
[d]Properties from GFPmut3.
[e]Referred to as ymNeonGreen$_{WT}$ throughout the manuscript.

2.3. Codon bias and RNA folding

The codon adaptive index (CAI) calculator (https://www.genscript.com/tools/rare-codon-analysis) was used to determine the CAI for each ymNeonGreen variant in *E. coli vs. S. cerevisiae.* CAI calculations were performed using the first 20 codons, of which 9 codons were changed to reduce secondary structure. RNA structure images and stabilities were calculated using default settings for the mfold web server [27], http://www.unafold.org/mfold/applications/rna-folding-form-v2.php. To be consistent with calculated folding energies reported in several previous studies of secondary RNA structure in *S. cerevisiae,* the default temperature of 37 °C was used to calculate maximum folding stability (ΔG, Gibbs free energy change for folding, kcal/mol). Lower ΔG values indicate increased stability of the secondary structure. Where multiple RNA structures were possible, free energies reported are for the most stable structure.

2.4. ymNeonGreen fluorescence detection

Yeast strains were diluted in 3 mL of SC-trp with 20 g/L glucose to an optical density (OD_{600}) of 0.01. All cultures were grown overnight in triplicate at 30 °C in a rotating drum at 80 rpm to an OD_{600} of 1. A 20 μL sample of each culture was transferred to single well of a black, clear-bottom, 96 well microplate (Corning; Corning, NY, USA) and 180 μL of fresh media was added. ymNeonGreen fluorescence and optical density were measured using a Synergy HTX Multi-Mode microplate reader (Biotek; Winooski, Vermont, USA). Fluorescence was measured using a 485/20 nm filter for excitation and a 580/20 nm filter for emission. Measurements were read from the top with a read height of 1 mm and gain set at 50. Fluorescence data were background-corrected and normalized to background-corrected OD_{600} (FLU/OD). Cells from remaining culture were collected for RT-PCR by centrifugation for 5 min at 5000 rpm and resuspended in 0.5 mL of RNA*later*™ (Ambion; Austin, Tx, USA).

Bacterial strains were grown overnight at 37 °C in a shaking incubator in 1 mL of LB medium plus ampicillin (LB_{amp}). The overnight culture was diluted into 200 μL of fresh 37 °C LB_{amp} medium to an optical density (OD_{595}) of 0.05. Quadruplicate 200 μL cultures were incubated at 37 °C in a black, clear-bottom, 96 well microplate for 4 h at 150 rpm. Fluorescence was measured as described above.

2.5. Quantitative RT-PCR

Cells were grown and collected by centrifugation as described above. Yeast cells were resuspended in 0.5 mL of RNA*later*™ and incubated at room temperature for 1 hour. Cells were collected again by centrifugation, supernatant removed, and stored at −80 °C. Total RNA from triplicate cultures was prepared using an RNeasy mini spin column (Qiagen; Hilden, Germany) and DNase treated with TURBO DNA-free (Ambion; Austin, TX, USA). Total RNA concentration was measured using a spectrophotometer (NanoDrop ND-1000, Thermo Scientific; Waltham, MA, USA) and diluted in water to 10 ng/μL. Three technical replicate RT-PCR reactions were performed from each of three biological replicates using a Rotor-Gene real-time PCR cycler (Qiagen), a QuantiNova SYBR® green RT-PCR kit (Qiagen), and 20 ng of total RNA. Primers used for ymNeonGreen mRNA measurement were (NG-F, 5′-TCGCTAAACCTATGGCTGCT-3′) and (NG-R, 5′-AAGGCCTTTTGCCATTCTTT-3′). Primers used for ACT1 mRNA measurement were (ACT1-F, 5′-GCCTTCTACGTTTCCATCCA-3′) and (ACT1-R, 5′-GGCCAAATCGATTCTCAAAA-3′). Primer efficiencies were determined using a serial, 2-fold dilution of RNA and each primer set was determined to be 100% efficient. ymNeonGreen measurements were normalized to *ACT1* mRNA using the $2^{-\Delta\Delta C}{}_{T}$ method [28].

3. Results and discussion

3.1. ymNeonGreen$_{RM}$ variant with reduced secondary RNA structure

Natural 5′ untranslated regions (UTRs) from *Saccharomyces cerevisiae* genes have evolved to be rich in adenine nucleotides and weakly-folded with an average ΔG of −4.3 kcal/mol [29–32]. Several studies in *S. cerevisiae* show that stable secondary structure in the 5′ UTR, and specifically near the start codon, is detrimental to protein expression, mainly due to inhibition of translation [20,21,33–35]. In trying to understand why mNeonGreen and the codon optimized variant ymNeonGreen$_{WT}$ expressed poorly in *S. cerevisiae* compared to its expression in other organisms, we looked for secondary RNA structure near the start codon. Yeast promoters used in previous studies (P_{PGK1}), as well as the two yeast promoters used in this study (P_{HXT7} and P_{CYC1}), had secondary structure present at nucleotides −50 to −1 with folding energies of −5.10, −5.20, and −5.20 kcal/mol, respectively (Supplemental Fig. 1.). These ΔG values are in the natural range of secondary structure stability for yeast promoters and are not likely to result in poor translation. Both mNeonGreen and ymNeonGreen$_{WT}$ form hairpin RNA structures with folding energies of −15.10 and −14.50 kcal/mol, respectively (Fig. 1). Protein translation in *S. cerevisiae* is sensitive to the presence of secondary structure and has been shown to be inhibited by RNA structures with folding free energies of approximately −10 kcal/mol [18–21]. To determine if the secondary structure in the ymNeonGreen$_{WT}$ mRNA was inhibiting expression, we changed the nucleotide sequence to reduce the secondary structure to −4.40 kcal/mol, which is comparable to natural *S. cerevisiae* 5′ UTRs (Fig.1).

In changing the nucleotide sequence, we kept the protein sequence identical to that of ymNeonGreen$_{WT}$ so differences in fluorescence could not be attributed to changes in quantum yield or protein stability. Eleven nucleotides, corresponding to 9 codons, were changed to make the RNA-modified (RM) variant, ymNeonGreen$_{RM}$. Most of the nucleotide changes were in the wobble base of the codon (Fig. 2). Approximately 63% of the mRNA sequence downstream of the start codon (nucleotides +1 to 51) of the ymNeonGreen$_{WT}$ ORF is part of secondary structure with a $\Delta G = -14.50$ kcal/mol. For the ymNeonGreen$_{RM}$ variant, only 27% of the downstream sequence is double-stranded. Additionally, the secondary structure ($\Delta G = -4.40$ kcal/mol) is split between two separate small RNA hairpins that do not include the start codon, instead of one large RNA hairpin including part of the start codon for ymNeonGreen$_{WT}$ (Fig. 1).

3.2. Expression of ymNeonGreen variants in Escherichia coli

Translation in prokaryotes initiates internally, with the ribosome binding site encompassing a 30-nucleotide window around the start codon. Translation initiation is inhibited by the presence of stable secondary RNA structure in this region ([15], and reviewed in [36]). Most of the mRNA sequence in the ribosome binding site is involved in secondary structure for ymNeonGreen$_{WT}$. To determine if this structure inhibits expression in *E. coli*, both ymNeonGreen variants were placed immediately downstream of the *lac* promoter that is present in the pRS series of shuttle vectors [23]. *E. coli* cells containing both ymNeonGreen variants showed fluorescence indicating that translation could proceed in the presence of secondary structure in the WT variant. Removal of the secondary structure resulted in a 3.8-fold increase in fluorescence (Table 4), indicating that the secondary RNA structure was negatively impacting expression in a bacterial expression system. The change in fluorescence with respect to folding energy observed (~ 0.4-fold change per kcal/mol difference) with ymNeonGreen$_{RM}$ expression is the same magnitude seen in a previous study investigating the effects of secondary mRNA structure on GFP expression in *E. coli* [15].

When changing codons to reduce RNA structure, effort was also made to substitute frequently used codons based on the *S. cerevisiae* codon usage table. As frequently used codons for the same amino acid

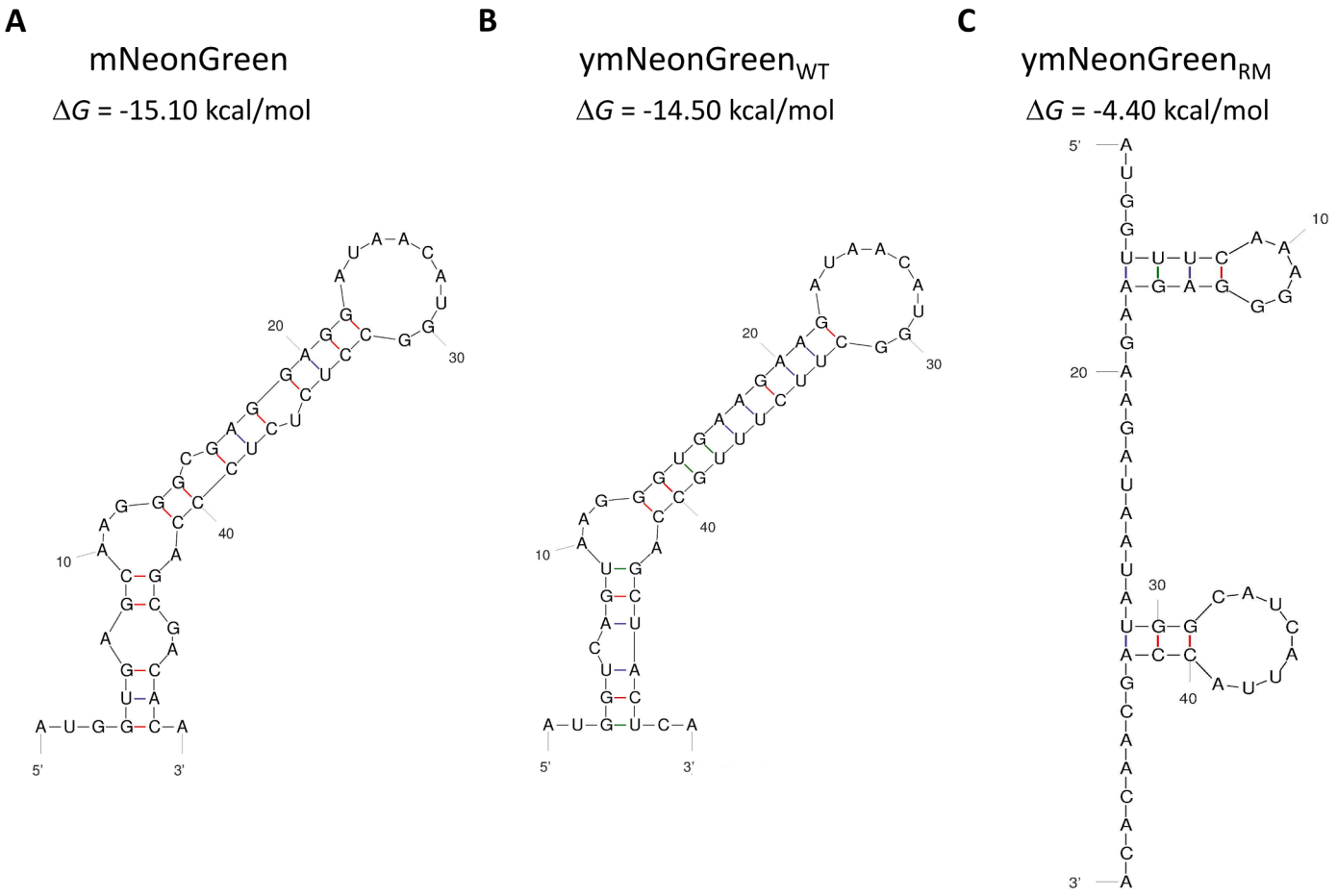

Fig. 1. Secondary RNA structures for mNeonGreen and ymNeonGreen variants. Δ*G* values were calculated using a temperature of 37 °C and represent the minimum folding energy (kcal/mol).

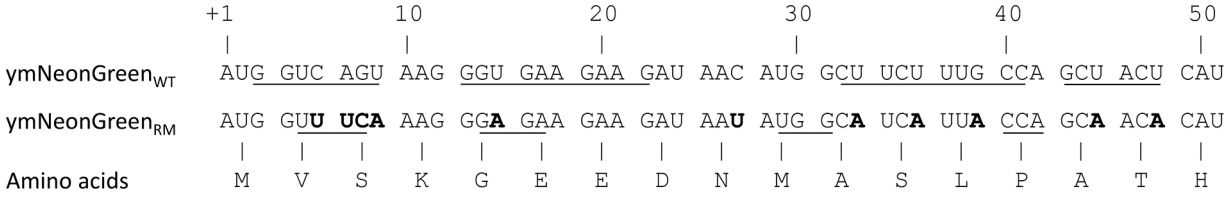

Fig. 2. Nucleotide alignment, changes, and involvement in secondary structure over the first 51 nucleotides of the ymNeonGreen ORF. Nucleotides in bold have been changed from the ymNeonGreen$_{WT}$ variant. Nucleotides underlined are part of secondary structure.

Table 4
Expression of ymNeonGreen variants in *E. coli*.

Reporter	RNA stability (Δ*G*, kcal/mol)	Fluorescence (FLU/OD$_{595}$)
ymNeonGreen$_{WT}$	−14.50	5,125 (±334)
ymNeonGreen$_{RM}$	−4.40	19,606 (±1,085)

Table 5
Codon bias for ymNeonGreen variants.

Strain used for bias calculation	CAI ymNeonGreen$_{WT}$	CAI ymNeonGreen$_{RM}$
E. coli	0.68	0.66
S. cerevisiae	0.91	0.89

CAI values were calculated for the first 20 amino acids of each variant. Nine codons were changed in the ymNeonGreen$_{RM}$ variant. CAI values for the entire ORF did not change (not shown).

were used for substitution, codon bias for the RNA structure modified ymNeonGreen$_{RM}$ variant was not significantly different (Table 5). CAI values calculated using the first 20 codons decreased slightly, while CAI values for the entire ORF did not change (not shown). Thus, increased fluorescence is not likely due to changes in codon bias.

3.3. Expression of ymNeonGreen variants in S. cerevisiae

Unlike translation initiation in prokaryotes, initiation for eukaryotes begins with the 40S ribosomal subunit binding at the 5′ 7^{m}GppN cap and scanning the mRNA 5′ to 3′ until the start codon is reached [36]. Secondary structure in the mRNA can inhibit translation either by blocking ribosome entry at the cap, or by impeding movement of the ribosome [16]. To evaluate the effect of RNA secondary structure near the start codon of ymNeonGreen$_{WT}$ on expression, we measured the fluorescence from both variants in *S. cerevisiae*. Two different promoters were used to compare the effect of differing upstream 5′ UTR sequences. The promoters also differed in strength, to determine if RNA structure in the

ymNeonGreen variants was more, or less, detrimental to expression when using weak promoters. The ymNeonGreen$_{RM}$ variant showed increased fluorescence from both a strong (P_{HXT7}) and a weak (P_{CYC1}) promoter compared to ymNeonGreen$_{WT}$ (Fig. 3). This result suggests that the strong secondary RNA structure localized 3′ of the start codon in the wild-type variant (see Fig. 1B) is the dominant structure that forms *in vivo* and is likely to result in reduced expression regardless of promoter used.

For comparison, fluorescence was also measured for *S. cerevisiae* cells expressing yEGFP3 [6], a traditional *A. victoria*-based enhanced GFP construct (pRH922), from the *HXT7* promoter. Cells expressing yEGFP3 had fluorescence levels of 9445 ± 941 FLU/OD. This level was identical to ymNeonGreen$_{WT}$ fluorescence and is consistent with previous reports that ymNeonGreen$_{WT}$ expression in yeast does not match the increased brightness predicted based on *in vitro* analysis and its expression level reported in multiple other organisms [8,13]. Our results suggest that poor performance of ymNeonGreen$_{WT}$ in yeast is attributable to the stable secondary RNA structure near the start codon.

The first seven amino acids of ymNeonGreen are identical to the leader sequence used in yEGFP3 (MVSKGEE), raising the possibility that yEGFP3 expression may also be limited by secondary RNA structure. The same region downstream of the yEGFP3 start codon (nucleotides 1–50) has a folding stability of −10.90 kcal/mol. The secondary structure however is split between two smaller RNA hairpins and does not include the yEGFP3 start codon (Supplemental Fig. 2). The larger of the two RNA hairpins (−7.20 kcal/mol) begins seven nucleotides 3′ of the start codon. Secondary RNA structure has been shown to inhibit translation more efficiently when close to the start codon [21]. Previous studies using the *CYC1* promoter showed that a −7.6 kcal/mol RNA hairpin immediately 5′ of the *CYC1* start codon could reduce expression 20-fold [18]. Given the stability and proximity of the RNA hairpin to the start codon of yEGFP3 (Supplemental Fig. 2), it may be possible to further improve yEGFP3 expression in *S. cerevisiae* by reducing the stability of this hairpin. As the focus of this study was on ymNeonGreen expression, we chose not to pursue these changes with yEGFP3.

3.4. Changes in mRNA level

Two recent genome-wide studies in *S. cerevisiae* showed significant positive correlation ($R = 0.95$ and $R = 0.93$, respectively) between steady state mRNA and protein levels [37,38]. Also, when analyzed at genome-scale, increased stability of secondary structure in the 5′-UTR has been shown to affect mRNA degradation, with strongly-folded 5′-UTR structures correlating with shorter mRNA half-life [39]. The interconnection of translation and mRNA degradation has been well-studied in *S. cerevisiae* (reviewed in [40]), and the decreased mRNA half-life is suggested to result from reduced translation [33,35,39,41–44]. Poor translation leads to increased mRNA deadenylation and decapping, resulting in less mRNA, most likely due to competition between the translation initiation complex and mRNA degradation machinery [35,42,45]. Based on this hypothesis, removing strong secondary structure in the 5′ UTR leads to increased translation and decreased deadenylation and decapping, resulting in higher mRNA levels. Thus, we would expect to see an increase in mRNA level if translation was enhanced for the ymNeonGreen$_{RM}$ variant. Quantitative RT-PCR analysis of the WT and RM variants, each expressed from two different promoters, was performed to compare ymNeonGreen mRNA levels. As expected, mRNA levels were lower in general for the weaker P_{CYC1} promoter. An increase in mRNA level was observed for ymNeonGreen$_{RM}$ compared to the ymNeonGreen$_{WT}$ for both promoters (Fig. 4).

Increased mRNA levels for the RM variant could result from either increased transcription of the mRNA or increased stability of the mRNA. mRNA degradation rates were not measured in this study, raising the possibility that transcription rates were higher. However, two different promoters showed an increase in mRNA level for the RM variant. Since the changes to the transcript were in the open reading frame and not in the promoter, we believe it is unlikely that the RM variant increased

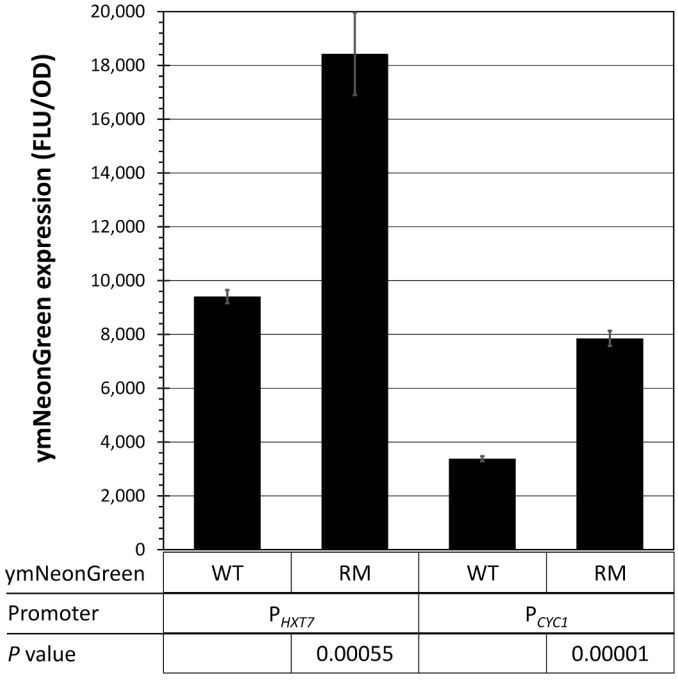

Fig. 3. Expression of ymNeonGreen variants in *S. cerevisiae*. ymNeonGreen expression in reported in fluorescence units per OD (FLU/OD). Fluorescence of cells expressing each ymNeonGreen variant was corrected for background fluorescence and normalized to culture density (OD). Data shown are the average expression for three biological replicates. Error bars represent the standard deviation.

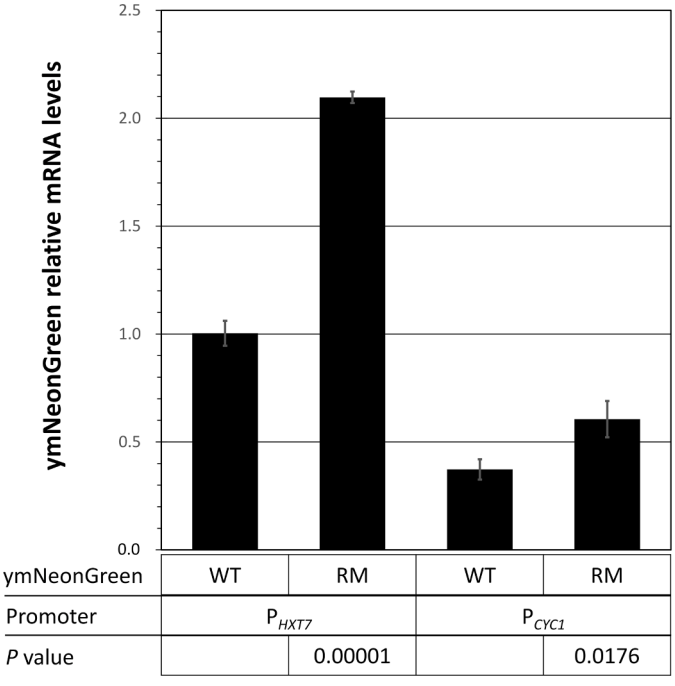

Fig. 4. Quantitative RT-PCR analysis for ymNeonGreen variants. Primers for ymNeonGreen amplified a region near the 3′ end of the ORF and were the same for both variants. mRNA concentrations for ymNeonGreen variants were normalized to *ACT1* mRNA levels using the $2^{-\Delta\Delta C_T}$ method and are shown relative to the strain expressing ymNeonGreen$_{WT}$ from the *HXT7* promoter. Data shown represents the average mRNA level for three biological replicates. Error bars represent the standard deviation.

transcription from both promoters. A more likely scenario is that the changes made to the RNA structure increased mRNA stability leading to its increased abundance. As numerous studies show that translation and mRNA stability are intrinsically linked in *S. cerevisiae* (reviewed in [40]), we believe the increase in mRNA level observed is the result of this interplay between mRNA degradation and translation.

3.5. Comparison of strong and weak promoters

Both strong (P_{HXT7}) and weak (P_{CYC1}) promoters were used in this study to determine if secondary RNA structure affected the promoters differently. With both promoters, ymNeonGreen fluorescence was increased by the removal of secondary structure (see Fig. 3). Fluorescence increased 2-fold when the *HXT7* promoter was used, compared to 2.3-fold when the *CYC1* promoter was used suggesting that secondary RNA structure may be more detrimental when a weak promoter is used. This result could stem from less frequent translation initiation from the weak promoter and/or decreased ribosome density. Both events would allow more time for formation of inhibitory secondary RNA structures from weak promoters.

It is also possible that translation capacity reaches a maximum for strong promoters and additional mRNA, while leading to increased protein levels, does not lead to more protein per mRNA. In two recent studies that show a genome-wide correlation between mRNA and protein level [37,38], expression appeared to saturate for genes with the highest mRNA levels. Saturation of expression for high abundance mRNAs was also observed in several studies investigating the effect of promoter:terminator combinations [46,47]. These studies showed that the effect of expression-enhancing terminator elements where greatest when using lower expression promoters. Conversely, the effect was minimized significantly for the highest expressing variants. Another study looking at the correlation between protein and mRNA abundance in yeast showed that protein/mRNA ratios were highly variable for low abundance mRNAs, but in general decreased with increased mRNA abundance [48]. We also measured protein/mRNA for our study by calculating the relative fluorescence normalized to relative mRNA concentration (FLU/mRNA, Fig. 5). FLU/mRNA values did not change between the two ymNeonGreen variants when using the stronger *HXT7* promoter. The *HXT7* promoter used in this study is a highly active, constitutive promoter, that was shown to be over 8-fold more active than several other glycolytic promoters [25]. We did see an increase in mRNA level for the RM variant but did not see a corresponding increase in fluorescence per mRNA. These data are consistent with saturation of expression for abundant mRNAs that has been observed in previous studies. In contrast, when using the weaker *CYC1* promoter, we observed that removing secondary RNA structure increased fluorescence per mRNA by 40%. The increase in fluorescence per mRNA from the *CYC1* promoter suggests that weak promoters are more susceptible than strong promoters to inhibition of expression by secondary RNA structure. While reducing RNA structure near the start codon was shown to increase expression from both promoters used in this study, additional investigation of mRNA decay rates and ribosome loading densities for the ymNeonGreen variants will provide further understanding of how expression was increased.

4. Conclusions

In summary, this study shows that $ymNeonGreen_{WT}$ expression in the budding yeast *S. cerevisiae* is limited by stable secondary RNA structure ($\Delta G = -14.50$ kcal/mol) immediately downstream of the start codon. Eliminating the RNA hairpin, while keeping the ymNeonGreen protein sequence the same, increased fluorescence of $ymNeonGreen_{RM}$ in both *S. cerevisiae* and in *E. coli* approximately 2-fold and 4-fold, respectively. The increase in fluorescence was seen for both weak and strong promoters in *S. cerevisiae*, further suggesting that changes made to remove RNA secondary structure immediately downstream of the

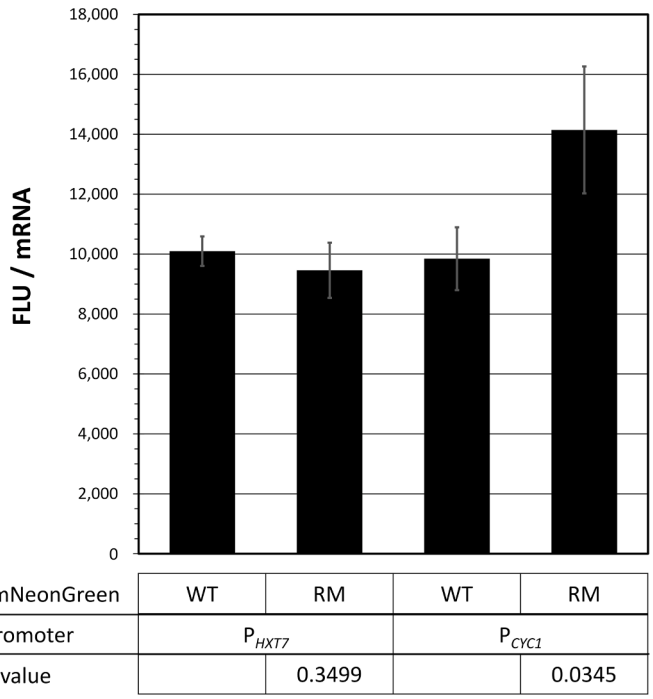

ymNeonGreen	WT	RM	WT	RM
Promoter	P_{HXT7}		P_{CYC1}	
P value		0.3499		0.0345

Fig. 5. Translation efficiency for ymNeonGreen variants. Translation efficiency is calculated as the relative amount of protein (*i.e.*, fluorescence) per mRNA and is shown as relative fluorescence units per relative mRNA level (FLU/mRNA). Data shown are the average expression for three biological replicates. Error bars represent the standard deviation.

$ymNeonGreen_{RM}$ start codon were responsible for the increase observed. Based on these results, we anticipate increased expression of $ymNeonGreen_{RM}$ to be seen regardless of *S. cerevisiae* promoter used. These results also highlight the importance of secondary RNA structure not only in the 5′-UTR, but also immediately 3′ of the start codon, when designing genes and reporter constructs for expression in *S. cerevisiae*.

Funding

This work was supported by the United States Department of Agriculture, Agricultural Research Service. Mention of trade names or commercial products in this publication is solely for the purpose of providing specific information and does not imply recommendation or endorsement by the U.S. Department of Agriculture. USDA is an equal opportunity provider and employer.

Author contributions

R.E.H. conceived the research, conducted experiments, and prepared the manuscript. J.A.M. and N.N.N contributed to experiment design, data analysis, and assisted in manuscript preparation. All authors read and approved the final manuscript.

Declaration of Competing Interest

The authors have no conflicts of interest to declare.

Acknowledgements

We thank Katherine Card for her technical assistance throughout this study.

Supplementary materials

Supplementary material associated with this article can be found, in the online version, at doi:10.1016/j.btre.2021.e00697.

References

[1] M. Chalfie, Y. Tu, G. Euskirchen, W.W. Ward, D.C. Prasher, Green fluorescent protein as a marker for gene expression, Science 263 (1994) 802–805, https://doi.org/10.1126/science.8303295.

[2] O. Shimomura, F.H. Johnson, Y. Saiga, Extraction, purification and properties of aequorin, a bioluminescent protein from the luminous hydromedusan, *Aequorea*, J. Cell Comp. Physiol. 59 (1962) 223–239, https://doi.org/10.1002/jcp.1030590302.

[3] E. Balleza, J.M. Kim, P. Cluzel, Systematic characterization of maturation time of fluorescent proteins in living cells, Nat. Methods 15 (2018) 47–51, https://doi.org/10.1038/nmeth.4509.

[4] B.P. Cormack, R.H. Valdivia, S. Falkow, FACS-optimized mutants of the green fluorescent protein (GFP), Gene 173 (1996) 33–38, https://doi.org/10.1016/0378-1119(95)00685-0.

[5] D.A. Zacharias, J.D. Violin, A.C. Newton, R.Y. Tsien, Partitioning of lipid-modified monomeric GFPs into membrane microdomains of live cells, Science 296 (2002) 913–916, https://doi.org/10.1126/science.1068539.

[6] B.P. Cormack, G. Bertram, M. Egerton, N.A. Gow, S. Falkow, A.J. Brown, Yeast-enhanced green fluorescent protein (yEGFP): a reporter of gene expression in *Candida albicans*, Microbiology 143 (1997) 303–311, https://doi.org/10.1099/00221287-143-2-303.

[7] N.C. Shaner, G.G. Lambert, A. Chammas, Y. Ni, P.J. Cranfill, M.A. Baird, B.R. Sell, J.R. Allen, R.N. Day, M. Israelsson, et al., A bright monomeric green fluorescent protein derived from *Branchiostoma lanceolatum*, Nat. Methods 10 (2013) 407–409, https://doi.org/10.1038/nmeth.2413.

[8] D. Botman, D.H. de Groot, P. Schmidt, J. Goedhart, B. Teusink, In vivo characterisation of fluorescent proteins in budding yeast, Sci. Rep. 9 (2019) 2234, https://doi.org/10.1038/s41598-019-38913-z.

[9] T.J. Lambert, FPbase: a community-editable fluorescent protein database, Nat. Methods 16 (2019) 277–278, https://doi.org/10.1038/s41592-019-0352-8.

[10] S. Ceolin, M. Hanf, M. Bozek, A.E. Storti, N. Gompel, U. Unnerstall, C. Jung, U. Gaul, A sensitive mNeonGreen reporter system to measure transcriptional dynamics in *Drosophila* development, Commun. Biol. 3 (2020) 663, https://doi.org/10.1038/s42003-020-01375-5.

[11] L. Hostettler, L. Grundy, S. Kaser-Pebernard, C. Wicky, W.R. Schafer, D.A. Glauser, The bright fluorescent protein mNeonGreen facilitates protein expression analysis in vivo, G3 (Bethesda) 7 (2017) 607–615, https://doi.org/10.1534/g3.116.038133.

[12] E. Tanida-Miyake, M. Koike, Y. Uchiyama, I. Tanida, Optimization of mNeonGreen for *Homo sapiens* increases its fluorescent intensity in mammalian cells, PLoS ONE 13 (2018), e0191108, https://doi.org/10.1371/journal.pone.0191108.

[13] M. Kaishima, J. Ishii, T. Matsuno, N. Fukuda, A. Kondo, Expression of varied GFPs in *Saccharomyces cerevisiae*: codon optimization yields stronger than expected expression and fluorescence intensity, Sci. Rep. 6 (2016) 35932, https://doi.org/10.1038/srep35932.

[14] M.H. de Smit, J. van Duin, Secondary structure of the ribosome binding site determines translational efficiency: a quantitative analysis, Proc. Natl. Acad. Sci. U. S. A. 87 (1990) 7668–7672, https://doi.org/10.1073/pnas.87.19.7668.

[15] G. Kudla, A.W. Murray, D. Tollervey, J.B. Plotkin, Coding-sequence determinants of gene expression in *Escherichia coli*, Science 324 (2009) 255–258, https://doi.org/10.1126/science.1170160.

[16] M. Kozak, Influences of mRNA secondary structure on initiation by eukaryotic ribosomes, Proc. Natl. Acad. Sci. U. S. A. 83 (1986) 2850–2854, https://doi.org/10.1073/pnas.83.9.2850.

[17] A.M. Cigan, E.K. Pabich, T.F. Donahue, Mutational analysis of the *HIS4* translational initiator region in *Saccharomyces cerevisiae*, Mol. Cell. Biol. 8 (1988) 2964–2975, https://doi.org/10.1128/mcb.8.7.2964.

[18] S.B. Baim, F. Sherman, mRNA structures influencing translation in the yeast *Saccharomyces cerevisiae*, Mol. Cell. Biol. 8 (1988) 1591–1601, https://doi.org/10.1128/mcb.8.4.1591.

[19] C.C. Oliveira, J.J. van den Heuvel, J.E. McCarthy, Inhibition of translational initiation in *Saccharomyces cerevisiae* by secondary structure: the roles of the stability and position of stem-loops in the mRNA leader, Mol. Microbiol. 9 (1993) 521–532, https://doi.org/10.1111/j.1365-2958.1993.tb01713.x.

[20] F.A. Sagliocco, M.R. Vega Laso, D. Zhu, M.F. Tuite, J.E. McCarthy, A.J. Brown, The influence of 5′-secondary structures upon ribosome binding to mRNA during translation in yeast, J. Biol. Chem. 268 (1993) 26522–26530, https://doi.org/10.1016/s0021-9258(19)74344-0.

[21] M.R. Vega Laso, D. Zhu, F. Sagliocco, A.J. Brown, M.F. Tuite, J.E. McCarthy, Inhibition of translational initiation in the yeast *Saccharomyces cerevisiae* as a function of the stability and position of hairpin structures in the mRNA leader, J. Biol. Chem. 268 (1993) 6453–6462, https://doi.org/10.1016/s0021-9258(18)53273-7.

[22] R.E. Hector, J.A. Mertens, N.N. Nichols, Development and characterization of vectors for tunable expression of both xylose-regulated and constitutive gene expression in *Saccharomyces* yeasts, N. Biotechnol. 53 (2019) 16–23, https://doi.org/10.1016/j.nbt.2019.06.006.

[23] R.S. Sikorski, P. Hieter, A system of shuttle vectors and yeast host strains designed for efficient manipulation of DNA in *Saccharomyces cerevisiae*, Genetics 122 (1989) 19–27, https://doi.org/10.1093/genetics/122.1.19.

[24] R.E. Hector, B.S. Dien, M.A. Cotta, N. Qureshi, Engineering industrial *Saccharomyces cerevisiae* strains for xylose fermentation and comparison for switchgrass conversion, J. Ind. Microbiol. Biotechnol. 38 (2011) 1193–1202, https://doi.org/10.1007/s10295-010-0896-1.

[25] J. Hauf, F.K. Zimmermann, S. Muller, Simultaneous genomic overexpression of seven glycolytic enzymes in the yeast *Saccharomyces cerevisiae*, Enz. Mic. Technol. 26 (2000) 688–698, https://doi.org/10.1016/s0141-0229(00)00160-5.

[26] T.W. Christianson, R.S. Sikorski, M. Dante, J.H. Shero, P. Hieter, Multifunctional yeast high-copy-number shuttle vectors, Gene 110 (1992) 119–122, https://doi.org/10.1016/0378-1119(92)90454-W.

[27] M. Zuker, Mfold web server for nucleic acid folding and hybridization prediction, Nuc. Acids Res. 31 (2003) 3406–3415, https://doi.org/10.1093/nar/gkg595.

[28] K.J. Livak, T.D. Schmittgen, Analysis of relative gene expression data using real-time quantitative PCR and the $2^{-\Delta\Delta CT}$ Method, Methods 25 (2001) 402–408, https://doi.org/10.1006/meth.2001.1262.

[29] M. Kertesz, Y. Wan, E. Mazor, J.L. Rinn, R.C. Nutter, H.Y. Chang, E. Segal, Genome-wide measurement of RNA secondary structure in yeast, Nature 467 (2010) 103–107, https://doi.org/10.1038/nature09322.

[30] T. Tuller, Y.Y. Waldman, M. Kupiec, E. Ruppin, Translation efficiency is determined by both codon bias and folding energy, Proc. Natl. Acad. Sci. U. S. A. 107 (2010) 3645–3650, https://doi.org/10.1073/pnas.0909910107.

[31] A. Robbins-Pianka, M.D. Rice, M.P. Weir, The mRNA landscape at yeast translation initiation sites, Bioinformatics 26 (2010) 2651–2655, https://doi.org/10.1093/bioinformatics/btq509.

[32] A. Mark Cigan, T.F. Donahue, Sequence and structural features associated with translational initiator regions in yeast — A review, Gene 59 (1987) 1–18, https://doi.org/10.1016/0378-1119(87)90261-7.

[33] S. Dvir, L. Velten, E. Sharon, D. Zeevi, L.B. Carey, A. Weinberger, Deciphering the rules by which 5′-UTR sequences affect protein expression in yeast, Proc. Natl. Acad. Sci. USA. 110 (2013), https://doi.org/10.1073/pnas.1222534110.

[34] T. LaGrandeur, R. Parker, The cis acting sequences responsible for the differential decay of the unstable MFA2 and stable PGK1 transcripts in yeast include the context of the translational start codon, RNA 5 (1999) 420–433, https://doi.org/10.1017/s1355838299981748.

[35] D. Muhlrad, C.J. Decker, R. Parker, Turnover mechanisms of the stable yeast *PGK1* mRNA, Mol. Cell. Biol. 15 (1995) 2145–2156, https://doi.org/10.1128/MCB.15.4.2145.

[36] M. Kozak, Regulation of translation via mRNA structure in prokaryotes and eukaryotes, Gene 361 (2005) 13–37, https://doi.org/10.1016/j.gene.2005.06.037.

[37] D.E. Weinberg, P. Shah, S.W. Eichhorn, J.A. Hussmann, J.B. Plotkin, D.P. Bartel, Improved ribosome-footprint and mRNA measurements provide insights into dynamics and regulation of yeast translation, Cell Rep. 14 (2016) 1787–1799, https://doi.org/10.1016/j.celrep.2016.01.043.

[38] G. Csardi, A. Franks, D.S. Choi, E.M. Airoldi, D.A. Drummond, Accounting for experimental noise reveals that mRNA levels, amplified by post-transcriptional processes, largely determine steady-state protein levels in yeast, PLos Genet. 11 (2015), e1005206, https://doi.org/10.1371/journal.pgen.1005206.

[39] M. Ringner, M. Krogh, Folding free energies of 5′-UTRs impact post-transcriptional regulation on a genomic scale in yeast, PLoS Comput. Biol. 1 (2005) e72, https://doi.org/10.1371/journal.pcbi.0010072.

[40] S. Huch, T. Nissan, Interrelations between translation and general mRNA degradation in yeast, Wiley Interdiscip Rev RNA 5 (2014) 747–763, https://doi.org/10.1002/wrna.1244.

[41] B.J. de la Cruz, S. Prieto, I.E. Scheffler, The role of the 5′ untranslated region (UTR) in glucose-dependent mRNA decay, Yeast 19 (2002) 887–902, https://doi.org/10.1002/yea.884.

[42] T. Sweet, C. Kovalak, J. Coller, The DEAD-box protein Dhh1 promotes decapping by slowing ribosome movement, PLoS Biol. 10 (2012), e1001342, https://doi.org/10.1371/journal.pbio.1001342.

[43] V. Presnyak, N. Alhusaini, Y.H. Chen, S. Martin, N. Morris, N. Kline, S. Olson, D. Weinberg, K.E. Baker, B.R. Graveley, et al., Codon optimality is a major determinant of mRNA stability, Cell 160 (2015) 1111–1124, https://doi.org/10.1016/j.cell.2015.02.029.

[44] B. Neymotin, V. Ettorre, D. Gresham, Multiple transcript properties related to translation affect mRNA degradation rates in *Saccharomyces cerevisiae*, G3 (Bethesda) 6 (2016) 3475–3483, https://doi.org/10.1534/g3.116.032276.

[45] D.C. Schwartz, R. Parker, Mutations in translation initiation factors lead to increased rates of deadenylation and decapping of mRNAs in *Saccharomyces cerevisiae*, Mol. Cell. Biol. 19 (1999) 5247–5256, https://doi.org/10.1128/MCB.19.8.5247.

[46] K.A. Curran, A.S. Karim, A. Gupta, H.S. Alper, Use of expression-enhancing terminators in *Saccharomyces cerevisiae* to increase mRNA half-life and improve gene expression control for metabolic engineering applications, Metab. Eng. 19 (2013) 88–97, https://doi.org/10.1016/j.ymben.2013.07.001.

[47] L. Wei, Z. Wang, G. Zhang, B. Ye, Characterization of terminators in *Saccharomyces cerevisiae* and an exploration of factors affecting their strength, ChemBioChem 18 (2017) 2422–2427, https://doi.org/10.1002/cbic.201700516.

[48] S.P. Gygi, Y. Rochon, B.R. Franza, R. Aebersold, Correlation between protein and mRNA abundance in yeast, Mol. Cell. Biol. 19 (1999) 1720–1730, https://doi.org/10.1128/MCB.19.3.1720.